



## Supporting Information

© Wiley-VCH 2015

69451 Weinheim, Germany

## **Particle Display: A Quantitative Screening Method for Generating High-Affinity Aptamers\*\***

*Jinpeng Wang, Qiang Gong, Nupur Maheshwari, Michael Eisenstein, Mary Luz Arcila, Kenneth S. Kosik, and H. Tom Soh\**

anie\_201309334\_sm\_miscellaneous\_information.pdf

## **Supplementary Information**

### **Methods**

#### **DNA preparation**

The single-stranded DNA (ssDNA) library, primers and selected aptamer sequences were purchased from Integrated DNA Technologies (IDT). The library was synthesized with hand mixing and PAGE-purified. Each 100-nucleotide (nt) library member featured a 60-nt randomized sequence flanked by 20-nt PCR primer sites (5'-AGCAGCACAGAGGTCAGATG-[60N]-CCTATGCGTGCTACCGTGAA-3'). Unlabeled, 5'-amino-modified and Alexa Fluor 647-modified PCR primers were obtained from IDT with HPLC purification.

#### **Coupling forward primers (FP) to particles:**

500  $\mu$ L of 1- $\mu$ m MyOne carboxylic acid magnetic particles ( $10^7/\mu$ L, Life Technologies) were washed once with 500  $\mu$ L of 0.01N NaOH and three times with 1 mL of nuclease-free water, then resuspended in a 150  $\mu$ L reaction mixture containing 200 mM NaCl, 0.2 mM 5'-amino-modified FP (5'-amino-PEG18-AGC AGC ACA GAG GTC AGA TG-3'), 1 mM imidazole chloride, 50% v/v dimethyl sulfoxide (DMSO) and 250 mM 1-ethyl-3-(3-dimethylaminopropyl)carbodiimide (EDC) (Pierce Biotechnology). Amino group modification enables covalent coupling, keeping FPs attached to the particles during thermal cycling, with the PEG18 at the 5' end serving as a spacer. Particles were mixed well with reagents, vortexed, sonicated and incubated overnight at room temperature (RT) on a rotator. The potential interactions among the aptamers on the particle surface are a concern because they could potentially reduce the diversity of available aptamers to interact with the target protein. In order to minimize these undesired interactions, we incorporated a PEG18 molecule as a spacer between the particle surface and the forward primer at the 5' end. After coupling the forward primer (FP), we passivated bead surfaces with PEG12 molecules to prevent non-specific binding of the target protein. We converted remaining carboxyls on the particles into amino-reactive NHS-ester in the presence of 250 mM EDC and 100 mM N-hydroxysuccinimide (NHS) in 2-(*N*-morpholino)ethanesulfonic acid (MES) buffer (100 mM, PH 4.7) (Pierce Biotechnology) for 30 minutes at RT, followed by conjugation with 20 mM amino-PEG12 (Pierce

Biotechnology) in MES buffer for one hour. The particles were washed four times with 500  $\mu$ L of TE buffer (10 mM Tris, pH 8.0, 0.1 mM EDTA), suspended in 500  $\mu$ L of TE buffer and stored at 4 °C.

To test conjugation efficiency, we incubated 1  $\mu$ M Alexa Fluor 647-modified FP complementary sequence (FPC) with 0.2  $\mu$ L of FP particles in 100  $\mu$ L of STE buffer (10 mM Tris pH 8.0, 50 mM NaCl, 1 mM EDTA) at 59 °C for 10 minutes, then snap cooled on ice for 2 minutes. The particles were washed twice with 100  $\mu$ L STE buffer and analyzed by Accuri C6 Flow Cytometer (BD Biosciences).

#### **AP synthesis:**

We generated our APs via emulsion PCR (1, 2). The oil phase (prepared fresh each day) was composed of 4.5% Span 80, 0.40% Tween 80 and 0.05% Triton X-100 in mineral oil, all purchased from Sigma-Aldrich. The aqueous phase consisted of 1× GoTaq PCR Master Mix (Promega), 25 mM MgCl<sub>2</sub>, 3.5 mM of each dNTP (Promega), 40 nM FP, 3  $\mu$ M reverse primer (RP), 0.25 U/ $\mu$ L of GoTaq Hot Start Polymerase (Promega), 2 pM template DNA, and 3 $\times$ 10<sup>8</sup> FP-coated particles in a total volume of 1 mL. Water-in-oil emulsions were prepared by adding 1 mL of the aqueous phase to 7 mL of oil phase in a DT-20 tube (IKA) locked into the Ultra-Turrax Device (IKA). This addition was performed drop-wise over 30 seconds while the mixture was being stirred at 900 rpm in the Ultra-Turrax. After adding the aqueous phase, we continued stirring the mixture for 5 min. The emulsions were distributed in 100  $\mu$ L aliquots into ~80 wells of a 96-well PCR plate. We performed PCR under the following cycling conditions: 95 °C for 3 min, followed by 50 cycles of 93 °C for 15 sec, 59 °C for 30 sec and 72 °C for 75 sec. After PCR, the emulsions were collected into an emulsion collection tray (Life Technologies) by centrifuging at 300 $\times$ g for 2 min. We broke the emulsion by adding 10 mL 2-butanol to the tray and transferred the collected sample to a 50 mL tube. After vortexing for 30 sec, the particles were pelleted by centrifugation at 3,500  $\times$  g for 5 min. After carefully removing the oil phase, we resuspended the particles in 1 mL of emulsion breaking (EB) buffer (100 mM NaCl, 1% Triton X-100, 10 mM Tris-HCl, pH 7.5, and 1 mM EDTA) and transferred them to a new 1.5 mL tube. After vortexing for 30 sec and centrifugation

for 90 sec at  $15,000 \times g$ , we removed the supernatant. We then placed the tube on a magnetic separator (MPC-S, Life Technologies), and pipetted off remaining supernatant. Particles were washed three times with TE buffer using magnetic separation, then resuspended in 300  $\mu\text{L}$  TE.

To generate ssDNA, we magnetically concentrated the particles for 1 min, and removed the supernatant with a pipette tip. We then resuspended the particles in 200  $\mu\text{L}$  of 0.1 M NaOH and incubated for 2 min. We placed the tube in the magnetic separator for 1 min and carefully removed the supernatant. After repeating this step twice, we resuspended the particles in 300  $\mu\text{L}$  TE.

The allocation patterns of template DNA and FP-coated particles during emulsion PCR roughly follows a Poisson distribution. The probability that there are exactly  $k$  DNA molecules or  $k$  FP-coated particles in one droplet is therefore equal to  $f(k;\lambda) = \lambda^k e^{-\lambda} / k!$ , where  $\lambda$  is the input DNA:droplet or particle:droplet ratio. Taking the template distribution as an example, the amount of DNA template used in the emulsion PCR is the key parameter affecting this outcome. Too little template results in too few positive particles, compromising the diversity of the particle population, while too much template results in too many droplets containing multiple templates (**Fig. S2b**). Based on the Poisson distribution, most particles are clonal when  $20 \pm 15\%$  of the particles contain PCR products (1, 2). To confirm this, we annealed APs with Alexa Fluor 647-labeled RP in STE buffer at 59 °C for 10 minutes and snap-cooled on ice for 2 minutes. The particles were then washed twice with 100  $\mu\text{L}$  STE buffer and analyzed by flow cytometry (**Fig. S2c**).

qPCR was performed with an iQ5 instrument (Bio-Rad) to estimate aptamer copy number for each AP. Calibration samples were prepared by adding  $10^6$ ,  $10^7$ ,  $10^8$ ,  $10^9$  or  $10^{10}$  templates into a 20  $\mu\text{L}$  reaction containing 250 nM each of FP and RP, 1,000 FP-coated particles, 10  $\mu\text{L}$  GoTaq PCR Master Mix (Promega) and 0.5× SYBR green (Life Technologies). Test samples were prepared identically, but with 1,000 APs. From the

threshold cycle, we quantified  $4.8 \times 10^7$  sequences on 1,000 APs (**Fig. S2d**). Since only 20% of APs displayed template sequences, the average copy number of sequences on each template-bearing AP was around  $2.4 \times 10^5$ .

### Biotinylation of protein targets:

We purchased the following (His)<sub>6</sub> tag-labeled protein targets: thrombin (Haematologic), ApoE (R&D Systems), 4-1BB (R&D Systems) and PAI-1 (Millipore). Proteins were biotinylated using the EZ-Link Micro NHS-PEO<sub>4</sub>-Biotinylation Kit (Pierce Biotechnology), which includes a polyethylene glycol (PEG) spacer to improve water-solubility. Protein concentrations were adjusted to 0.5 mg/mL with phosphate-buffered saline (PBS) prior to biotinylation. We typically used 50-fold molar excess of biotin reagent to label 50-100 µg protein for 30 minutes at RT, and removed free biotin via Zeba Desalt Spin Column (0.5 mL, Pierce Biotechnology). We measured biotinylated protein concentration based on absorbance at 280 nm using a NanoDrop spectrophotometer (Thermo Scientific).

### Particle display screening:

Prior to the screen, we used fluorescently labeled target to measure non-specific binding to FP-coated particles. ~80% of the APs after emulsion PCR are predicted to display only the FP on their surface based on Poisson statistics, and thus should not exhibit significant binding to the protein targets. FP displaying particles thus serve as an excellent negative control for establishing the “reference gate” to calibrate non-specific binding for the particle display screen (Fig. 2, red). During each round of screening, we incubated  $\sim 10^8$  APs in 2 mL of PBSMCT (DPBS with 2.5 mM MgCl<sub>2</sub>, 1 mM CaCl<sub>2</sub>, 0.05% TWEEN-20) with biotinylated proteins, then washed and incubated them with 50 nM streptavidin-phycoerythrin (SAPE) conjugate (Life Technologies) for 10 minutes. It is important to limit the incubation time with SAPE to decrease enrichment for aptamers that bind SAPE. Target concentrations used for each protein are listed in **Table S1**. SAPE labeling allowed us to isolate APs retaining the highest levels of fluorescence via flow cytometry. Based on our theoretical analysis, we set the sort gate at  $F_{max}/3$  and monitored the fluorescence distribution of APs at a range of different target concentrations and chose

the target concentration at which ~0.1% of the APs resided in the sort gate. Furthermore, to ensure that our selected aptamers indeed bind to the native protein, we also performed the following controls. First, before each round of FACS, we confirmed that aptamer particles do not bind to the streptavidin-fluorophore conjugate. Second, we used an alternative means of fluorescent labeling, such as coupling His-tagged protein with anti-His antibodies, to ensure that our aptamers recognize non-biotinylated versions of the protein. We then chose the reaction volume such that target binding to particle-displayed aptamers would not occur under depleting conditions, meaning most target molecules remain unbound and free in solution after the reaction reaches equilibrium. After collecting the highest-fluorescence APs by FACS, we PCR amplified the isolated aptamers to generate an enriched pool for a subsequent round of AP synthesis. After three rounds of screening and amplification for each target, we estimated the average  $K_d$  of the R3 pool by measuring mean fluorescence of all APs outside the reference gate at different  $[T]$ , and determined the  $[T]$  at which the mean fluorescence of this population was equal to  $(F_{max} + F_{bg})/2$ , the average  $K_d$  of the pool.

### **Particle PCR:**

After cloning and sequencing (3), we performed particle PCR to synthesize APs displaying each unique aptamer sequence. Each particle PCR reaction (100  $\mu$ L) consisted of 1× GoTaq PCR Master Mix (Promega), 25 mM MgCl<sub>2</sub>, 2  $\mu$ M Alexa Fluor 647-modified reverse primer (RP), 10 nM aptamer template and 5×10<sup>7</sup> FP-coated particles. PCR was carried out under the following cycling conditions: 95 °C for 3 min, followed by 28 cycles of 93 °C for 15 sec, 59 °C for 30 sec and 72 °C for 45 sec. To avoid particle aggregation and increase particle PCR efficiency, we vortexed and sonicated the reaction every four cycles after the 93 °C denaturing step. We then measured AP fluorescence intensity, using FACS to test particle PCR efficiency (**Fig. S2a**). After confirming that individual sequences were successfully amplified on APs, we removed the reverse strands as described above.

### **Characterization of individual aptamers and $K_d$ measurement:**

We quantified the relative binding affinities of selected aptamer candidates from each screen using a bead-based fluorescence binding assay. Different APs obtained from particle PCR, each displaying a unique sequence, were incubated with target at a single concentration. We used a non-binding FP-displaying particle as a negative control in each measurement (**Fig. S3**). We chose the best candidate aptamer for each target for further analysis and determination of  $K_d$  using a bead-based fluorescence binding assay (3).

### Theoretical basis of particle display

Particle display exploits the fact that each AP's fluorescence intensity is proportional to the target affinity of the aptamer displayed on its surface. Quantitatively, the mean fluorescence intensity ( $F$ ) of an AP displaying an aptamer with an equilibrium dissociation constant of  $K_d$  can be expressed as

$$F = \frac{[T]}{[T] + K_d} \times (F_{max} - F_{bg}) + F_{bg} \quad \text{Eq. S1}$$

where  $[T]$  is the concentration of the fluorescently-labeled target,  $F_{bg}$  is the mean background fluorescence of the APs, and  $F_{max}$  is the maximum mean fluorescence when an AP is saturated with labeled target (4–6). Thus, if we consider a population of APs and rank them ( $\text{AP}^i, i = 1, 2, \dots, n$ ) according to the affinity of the aptamers displayed on their surfaces (*i.e.*,  $K_d^1 < K_d^2 < \dots < K_d^n$ ), wherein  $\text{AP}^1$  is the particle displaying the highest affinity aptamer, then  $F^1 > F^2 > \dots > F^n$ . Because FACS employs logarithmic amplification electronics (6–8), the fluorescence signal is presented on a logarithmic scale. Therefore, on a FACS plot, the separation between  $\text{AP}^1$  and any other  $\text{AP}^i$  corresponds to the ratio of their mean fluorescence,  $Fr^i$ :

$$Fr^i = \frac{F^1}{F^i} = \frac{\left(\frac{[T]}{K_d^1}\right)^2 + \left(\frac{F_{bg}}{F_{max}} + \frac{K_d^i}{K_d^1}\right)\frac{[T]}{K_d^1} + \frac{F_{bg}}{F_{max}}\frac{K_d^i}{K_d^1}}{\left(\frac{[T]}{K_d^1}\right)^2 + \left(1 + \frac{F_{bg}}{F_{max}}\frac{K_d^i}{K_d^1}\right)\frac{[T]}{K_d^1} + \frac{F_{bg}}{F_{max}}\frac{K_d^i}{K_d^1}} \quad (i = 1, 2, \dots, n) \quad \text{Eq. S2}$$

Importantly, we note that  $Fr^i$  is dependent on one experimentally measurable system constant,  $F_{max}/F_{bg}$ , and two dimensionless variables,  $[T]/K_d^1$  and  $K_d^i/K_d^1 \equiv K_d r^i$ . Thus, for a given  $K_d r^i$ ,  $[T]/K_d^1$  is the only variable that determines both  $Fr^i$  and  $F^i$ . In our experimental system, we measured  $F_{max}$  and  $F_{bg}$  to be 7500 a.u. and 250 a.u., respectively. Using these values, we plotted  $Fr^i$  as a function of  $F^1/F_{max}$  for a range of  $2 < K_d r < 10$  (**Fig. S1a**). We observe that as  $F^1$  increases,  $Fr^i$  increases until it reaches an optimal value,  $(F^1)_{opt}^i$ , after which it decreases monotonically to 1.

Effective isolation of aptamers with the highest target affinity requires maximum

separation between AP<sup>1</sup> and AP<sup>*i*</sup>. To identify the  $(F^1)_{opt}^i$  that yields this condition, we first analysed the optimal  $[T]/K_d^1$  that results in maximum  $Fr^i$ . To do so, we took the derivative of Eq. S2 with respect to  $[T]$  and let it equal 0. The solution to this equation is

$$\left(\frac{[T]}{K_d^1}\right)_{opt}^i = \sqrt{\frac{F_{bg}}{F_{max}} K_d r^i} \quad (i=1,2,\dots,n) \quad \text{Eq. S3}$$

Next, we calculated  $(F^1)_{opt}^i$  by substituting Eq. S3 into Eq. S1.

$$(F^1)_{opt}^i = \frac{1 + \sqrt{\frac{F_{bg}}{F_{max} K_d r^i}}}{1 + \sqrt{\frac{F_{max}}{F_{bg} K_d r^i}}} F_{max} \quad (i=1,2,\dots,n) \quad \text{Eq. S4}$$

Using Eq. S4, we calculated the analytical solution of  $(F^1)_{opt}^i$  for a range of  $2 < K_d r < 10$  to be  $0.23 < (F^1)_{opt}^i / F_{max} < 0.38$  (denoted by \* in **Fig. S1a**). We chose this narrow range near  $K_d^1$  because effective isolation of AP<sup>1</sup> in this range would ensure exclusion of APs with larger  $K_d r$ , for which affinity is unacceptably low. We note that setting  $F^1 \approx F_{max}/3$  is a useful experimental guideline, ensuring that  $Fr^i$  is within 2% of the optimal value for APs in the range of  $2 < K_d r < 10$ , enabling maximum separation between AP<sup>1</sup> and AP<sup>*i*</sup>.

Next, we calculated the enrichment performance after one round of particle display screening. To do so, we first measured the fluorescence distribution of our APs and verified that the distribution was indeed log-normal as previously reported (6, 8). Thus, the fluorescence distribution of each AP<sup>*i*</sup> can be defined by the mean fluorescence ( $F^i$ ) and the coefficient of variance ( $CV^i$ ), which represents the variability of the fluorescence distribution. We determined the  $[T]$  that results in  $F^1 = F_{max}/3$ , and substituted this  $[T]$  into Eq. S1 to calculate  $F^i$ . We experimentally determined the  $CV^i$  to be 25% from FACS measurements. From these values, we obtained the fluorescence distribution of the APs (**Fig. S1b**). Next, we set the sort gate at  $F_{max}/3$ , and calculated the fraction of AP<sup>*i*</sup> whose fluorescence exceeds that threshold (**Fig. S1b**, shaded) and would therefore be collected by FACS. Finally, we obtained the enrichment of AP<sup>1</sup> over AP<sup>*i*</sup> by taking the ratio of the collected AP<sup>1</sup> and AP<sup>*i*</sup> (**Fig. 2b**).

## Supplementary Figures

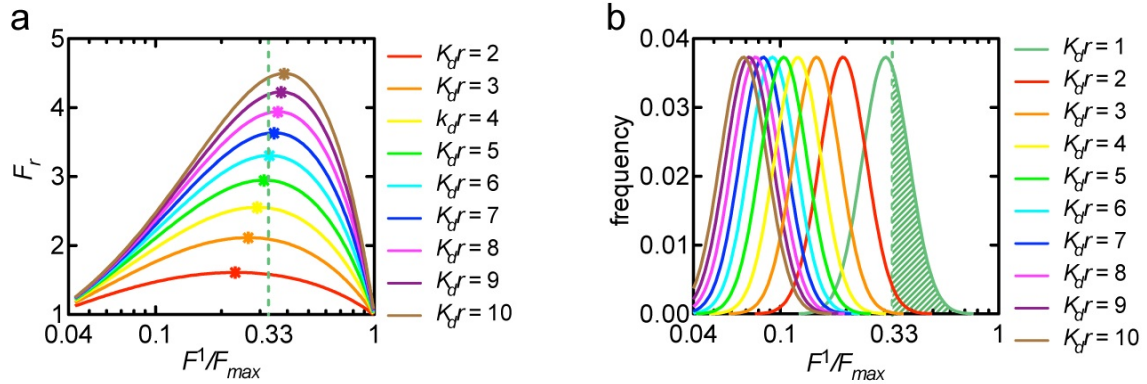


**Figure S1** Theoretical analysis. (a) The fluorescence intensity ratio ( $Fr$ ) of  $AP^1/AP^i$  ( $K_d r^i = 2, 3, \dots, 10$ ) plotted as a function of  $F^1/F_{max}$ . The optimal value for ( $F^1/F_{max}$ ) shifts from 0.23 to 0.38 as  $K_d r$  increases. Setting  $F^1 = F_{max}/3$  ensures that  $Fr^i$  is within 2% of the optimal value for APs where  $2 < K_d r < 10$ , enabling maximum separation between  $AP^1$  and  $AP^i$ . (b) Fluorescence distribution of  $AP^1$  and  $AP^i$  (log-normal probability density function with CV of 25%). When  $F^1 = F_{max}/3$ , the shaded region represents the fraction of  $AP^i$  whose fluorescence exceeds the threshold and is collected by FACS.

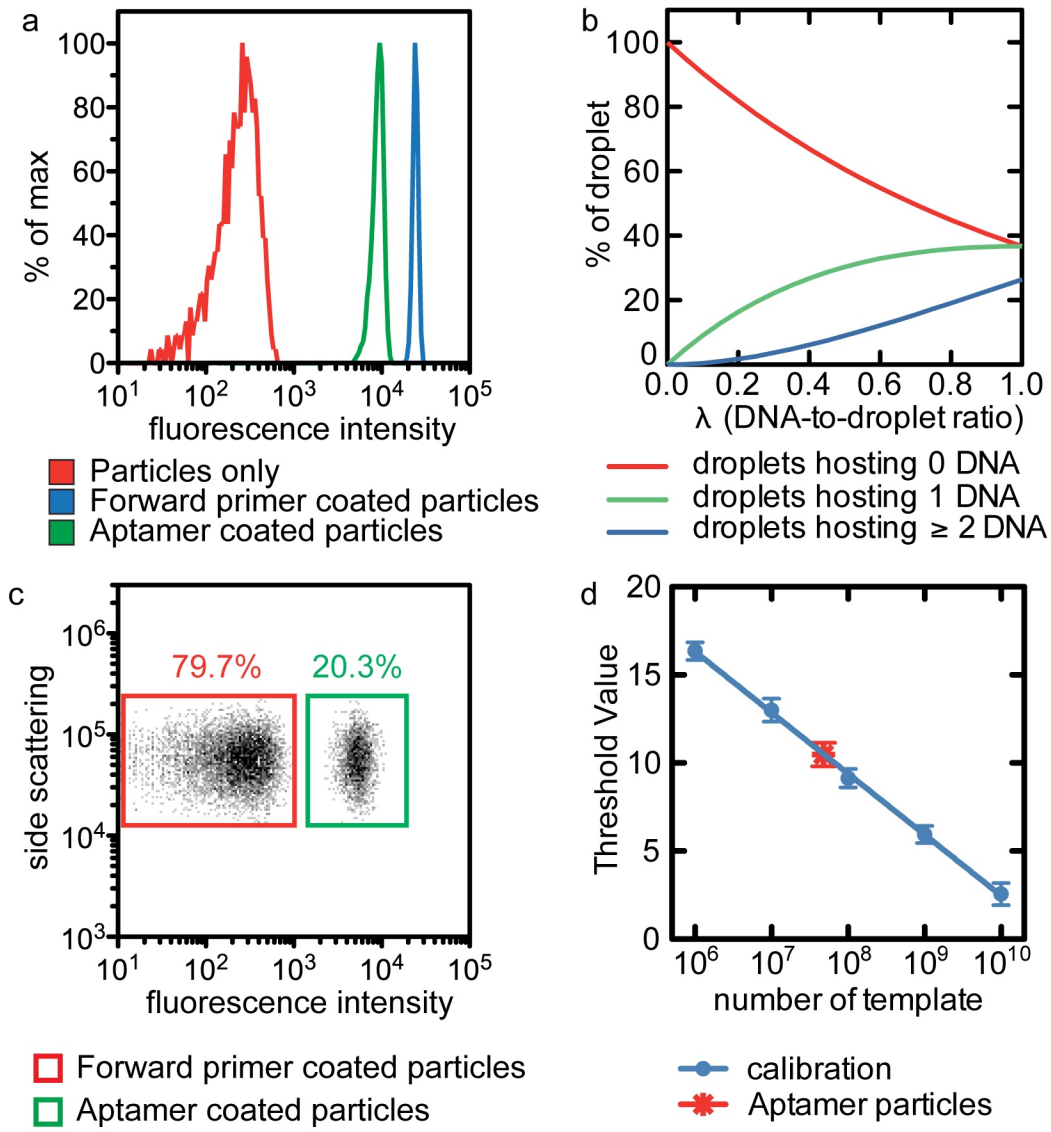


**Figure S2:** Aptamer particle synthesis. (a) Typical FACS histogram of singlet particles (red), FP-coated singlet particles hybridized with an Alexa Fluor 647-labeled FP complementary probe (blue), and ssDNA-displaying singlet particles hybridized with Alexa Fluor 647-labeled RP after particle PCR (green). (b) Effect of total template DNA number on the range of template copies per droplet, assuming Poisson distribution. When template DNA number is equal to the number of droplets, roughly 37% of droplets host no template DNA at all, whereas approximately 26% of droplets host two or more different templates. Since no more than one template molecule should be present per droplet, total template DNA copy number should be kept below 30% – and ideally at 20% – of the total droplet number to minimize the formation of non-clonal particles. (c) A typical FACS dot plot of singlet particles after emulsion PCR and annealing with Alexa Fluor 647-labeled RP. 20.3% of the particles contained PCR products, indicating that most particles

were clonal according to Poisson distribution. (d) qPCR was performed to quantify aptamer copy number for each AP. Threshold cycle values are plotted as a function of template number.

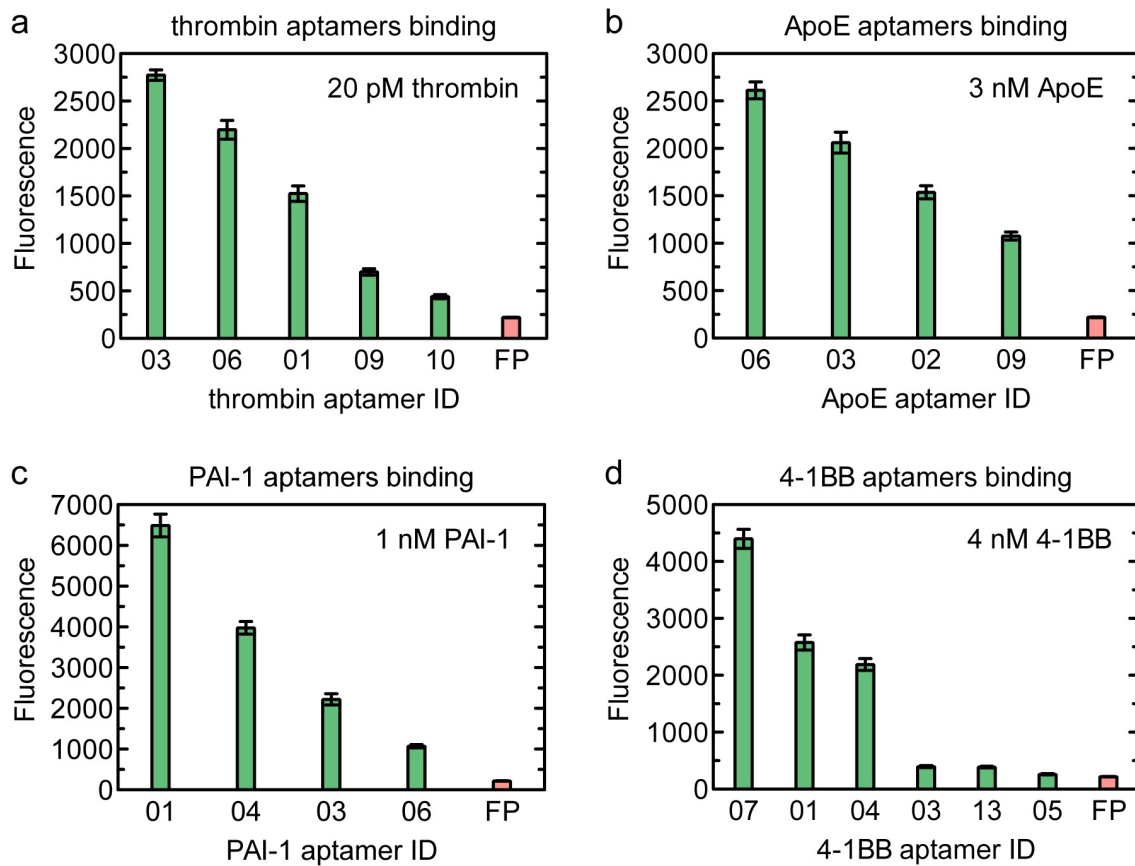


**Figure S3:** Aptamer target binding. We quantified the relative binding affinities of selected aptamer candidates from each screen using a bead-based fluorescence binding assay (3). Different APs, each displaying a unique aptamer sequence, were incubated with target at a single concentration. FP indicates a non-binding forward primer-displaying particle included as a negative control in each measurement. We chose the best candidate aptamer for each target for further analysis and determination of equilibrium dissociation binding constant ( $K_d$ ). (a) Thrombin aptamers with [thrombin] = 20 pM. (b) ApoE aptamers with [ApoE] = 3 nM. (c) PAI-1 aptamers with [PAI-1] = 1 nM. (d) 4-1BB aptamers with [4-1BB] = 4 nM.

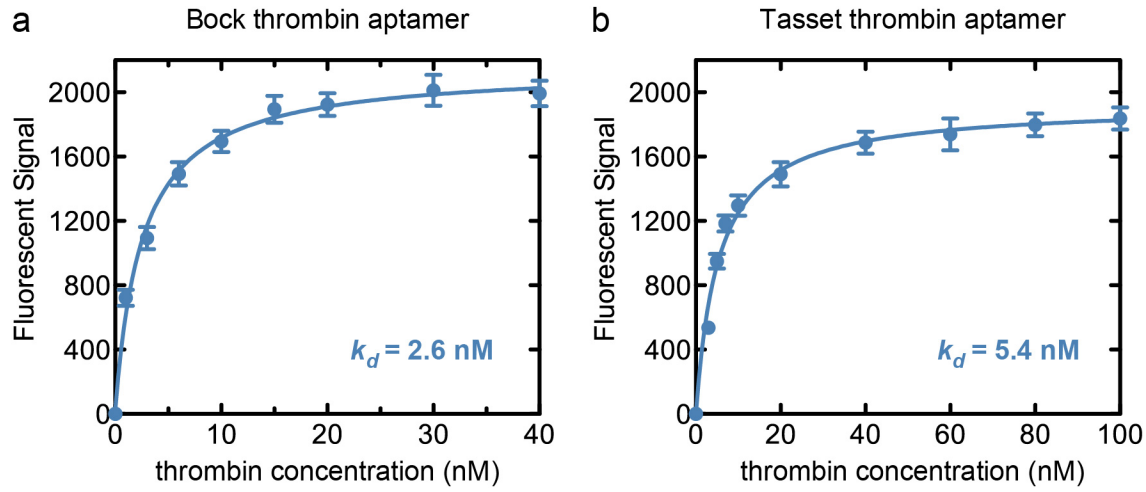


**Figure S4:** Affinity of previously published aptamers to thrombin. Bead-based fluorescence binding data for previously published (a) Bock (9) and (b) Tasset (10) thrombin aptamers showing measured  $K_d$  of 2.6 nM and 5.4 nM, respectively.

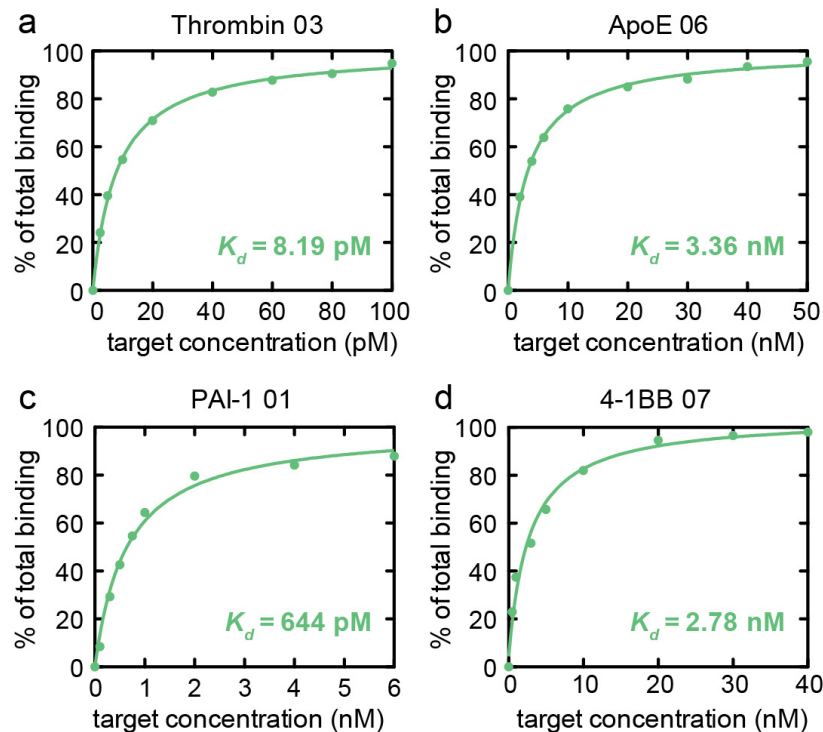


**Figure S5:**  $K_d$  measurement of the highest affinity aptamers using an alternative method wherein we immobilized target proteins (a) thrombin, (b) ApoE, (c) PAI-1 and (d) 4-1BB on magnetic beads, incubated with fluorescently-labeled aptamers at varying concentrations, and measured their fluorescence. As expected, the affinities obtained in this manner were in agreement with the results shown in Figure 3.

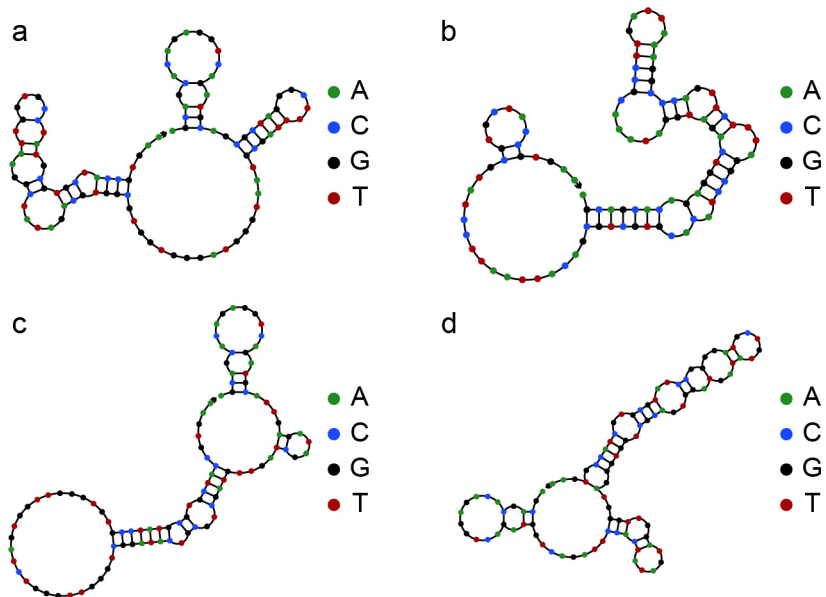


**Figure S6:** Secondary structures of the highest affinity aptamers for (a) thrombin, (b) ApoE, (c) PAI-1 and (d) 4-1BB as modeled by mfold (11).

**Table S1 | Experimental conditions for particle display.**

Target	[T]	# of AP sorted	# of AP collected	[T]	# of AP sorted	# of AP collected	[T]	# of AP sorted	# of AP collected
Thrombin	1 nM	$10^8$	$1.1 \times 10^5$	100 pM	$10^7$	$1.5 \times 10^4$	10 pM	$6 \times 10^6$	$1.0 \times 10^4$
ApoE	30 nM	$10^8$	$1.3 \times 10^5$	10 nM	$10^7$	$1.0 \times 10^4$	1 nM	$9 \times 10^6$	$1.3 \times 10^4$
PAI-1	40 nM	$10^8$	$1.2 \times 10^5$	10 nM	$10^7$	$9.4 \times 10^3$	400 pM	$8 \times 10^6$	$1.4 \times 10^4$
4-1BB	200 nM	$10^8$	$1.4 \times 10^5$	20 nM	$10^7$	$1.3 \times 10^4$	1 nM	$5 \times 10^6$	$9.2 \times 10^3$
particle display Round 1				particle display Round 2				particle display Round 3	

**Table S2 | Selected aptamer sequences.**

Clone ID	Selected region (5' to 3')
Thrombin 01	AAG TAGG TAT GTTTTTGGG TAGGG TGG TCG AG TTT GCA T TT GCT G CTT GG CG AG CAG C
Thrombin 02	AAG TAGG TAT GTTTTTGGG TAGGG TGG TCG AG TTT GCA T TT GCT G CTT GG CG AG CAG C
Thrombin 05	AAG TAGG TAT GTTTTTGGG TAGGG TGG TCG AG TTT GCA T TT GCT G CTT GG CG AG CAG C
Thrombin 13	AAG TAGG TAT GTTTTTGGG TAGGG TGG TCG AG TTT GCA T TT GCT G CTT GG CG AG CAG C
Thrombin 16	AAG TAGG TAT GTTTTTGGG TAGGG TGG TCG AG TTT GCA T TT GCT G CTT GG CG AG CAG C
Thrombin 03	CAG CG CTAGGGCTTTAGCGTAATGGG TAGGG TGG TG CGGTG CAG A T A TCGGA ATTGGTG
Thrombin 04	CAG CG CTAGGGCTTTAGCGTAATGGG TAGGG TGG TG CGGTG CAG A T A TCGGA ATTGGTG
Thrombin 07	CAG CG CTAGGGCTTTAGCGTAATGGG TAGGG TGG TG CGGTG CAG A T A TCGGA ATTGGTG
Thrombin 12	CAG CG CTAGGGCTTTAGCGTAATGGG TAGGG TGG TG CGGTG CAG A T A TCGGA ATTGGTG
Thrombin 14	CAG CG CTAGGGCTTTAGCGTAATGGG TAGGG TGG TG CGGTG CAG A T A TCGGA ATTGGTG
Thrombin 17	CAG CG CTAGGGCTTTAGCGTAATGGG TAGGG TGG TG CGGTG CAG A T A TCGGA ATTGGTG
Thrombin 19	CAG CG CTAGGGCTTTAGCGTAATGGG TAGGG TGG TG CGGTG CAG A T A TCGGA ATTGGTG
Thrombin 20	CAG CG CTAGGGCTTTAGCGTAATGGG TAGGG TGG TG CGGTG CAG A T A TCGGA ATTGGTG
Thrombin 06	TCGG TAGGGTACCTACTGAGGTACATA TATGGG TAGGG TGG TG CCG GT CC GG GA ATT CG TTT AA
Thrombin 08	TCGG TAGGGTACCTACTGAGGTACATA TATGGG TAGGG TGG TG CCG GT CC GG GA ATT CG TTT AA
Thrombin 11	TCGG TAGGGTACCTACTGAGGTACATA TATGGG TAGGG TGG TG CCG GT CC GG GA ATT CG TTT AA
Thrombin 15	TCGG TAGGGTACCTACTGAGGTACATA TATGGG TAGGG TGG TG CCG GT CC GG GA ATT CG TTT AA
Thrombin 18	TCGG TAGGGTACCTACTGAGGTACATA TATGGG TAGGG TGG TG CCG GT CC GG GA ATT CG TTT AA
Thrombin 09	AAGGCA CGAAATGGTTGGGGTGGATG TAGGGGTGCCTCGAGGACCGTTTTCTATAAAGA
Thrombin 10	CTAGACGTGCGAAGAGGTACTTATTG TGGTTGGG TGGTTCTCGCTCGTAGCGATTAGGG

Clone ID	Selected region (5' to 3')
ApoE 01	TTG TGG TTGGAGGGGGGGGGGGCTTGTGGCGGGCTTTGCCATGTCCTTGAGAAATCGTAGCAA
ApoE 09	TTG TGG TTGGAGGGGGGGGGGGCTTGTGGCGGGCTTTGCCATGTCCTTGAGAAATCGTAGCAA
ApoE 02	TTGGGGTTGGTGGGGGGGGGGGGCTTGTGGCGCTTAGACGTCGCTGCGAATTCTGACTG
ApoE 04	TTGGGGTTGGTGGGGGGGGGGGGCTTGTGGCGCTTAGACGTCGCTGCGAATTCTGACTG
ApoE 07	TTGGGGTTGGTGGGGGGGGGGGGCTTGTGGCGCTTAGACGTCGCTGCGAATTCTGACTG
ApoE 14	TTGGGGTTGGTGGGGGGGGGGGGCTTGTGGCGCTTAGACGTCGCTGCGAATTCTGACTG
ApoE 17	TTGGGGTTGGTGGGGGGGGGGGGCTTGTGGCGCTTAGACGTCGCTGCGAATTCTGACTG
ApoE 20	TTGGGGTTGGTGGGGGGGGGGGGCTTGTGGCGCTTAGACGTCGCTGCGAATTCTGACTG
ApoE 03	CAG TCCCATTCTGGGAGGGTTGGATTTACGGGGTGGAGCCCGGAGTG TGGGG TGCGGGG
ApoE 05	CAG TCCCATTCTGGGAGGGTTGGATTTACGGGGTGGAGCCCGGAGTG TGGGG TGCGGGG
ApoE 10	CAG TCCCATTCTGGGAGGGTTGGATTTACGGGGTGGAGCCCGGAGTG TGGGG TGCGGGG
ApoE 11	CAG TCCCATTCTGGGAGGGTTGGATTTACGGGGTGGAGCCCGGAGTG TGGGG TGCGGGG
ApoE 13	CAG TCCCATTCTGGGAGGGTTGGATTTACGGGGTGGAGCCCGGAGTG TGGGG TGCGGGG
ApoE 15	CAG TCCCATTCTGGGAGGGTTGGATTTACGGGGTGGAGCCCGGAGTG TGGGG TGCGGGG
ApoE 06	GATAAACGCCTTGATTAAGGCCAGTTCTTAGGCCTACACGTGCTGCGACATTAATT
ApoE 08	GATAAACGCCTTGATTAAGGCCAGTTCTTAGGCCTACACGTGCTGCGACATTAATT
ApoE 12	GATAAACGCCTTGATTAAGGCCAGTTCTTAGGCCTACACGTGCTGCGACATTAATT
ApoE 16	GATAAACGCCTTGATTAAGGCCAGTTCTTAGGCCTACACGTGCTGCGACATTAATT
ApoE 18	GATAAACGCCTTGATTAAGGCCAGTTCTTAGGCCTACACGTGCTGCGACATTAATT
ApoE 19	GATAAACGCCTTGATTAAGGCCAGTTCTTAGGCCTACACGTGCTGCGACATTAATT

**Table S2 | Selected aptamer sequences (continued).**

Clone ID	Selected region (5' to 3')
PAI-1 01	CATTGAGA TAGCTAGTTGTAGCTGCGTCATAGGCTGGGTTGGGTCTAGTGGTTGGGTGTG
PAI-1 02	CATTGAGA TAGCTAGTTGTAGCTGCGTCATAGGCTGGGTTGGGTCTAGTGGTTGGGTGTG
PAI-1 07	CATTGAGA TAGCTAGTTGTAGCTGCGTCATAGGCTGGGTTGGGTCTAGTGGTTGGGTGTG
PAI-1 10	CATTGAGA TAGCTAGTTGTAGCTGCGTCATAGGCTGGGTTGGGTCTAGTGGTTGGGTGTG
PAI-1 11	CATTGAGA TAGCTAGTTGTAGCTGCGTCATAGGCTGGGTTGGGTCTAGTGGTTGGGTGTG
PAI-1 12	CATTGAGA TAGCTAGTTGTAGCTGCGTCATAGGCTGGGTTGGGTCTAGTGGTTGGGTGTG
PAI-1 14	CATTGAGA TAGCTAGTTGTAGCTGCGTCATAGGCTGGGTTGGGTCTAGTGGTTGGGTGTG
PAI-1 17	CATTGAGA TAGCTAGTTGTAGCTGCGTCATAGGCTGGGTTGGGTCTAGTGGTTGGGTGTG
PAI-1 18	CATTGAGA TAGCTAGTTGTAGCTGCGTCATAGGCTGGGTTGGGTCTAGTGGTTGGGTGTG
PAI-1 19	CATTGAGA TAGCTAGTTGTAGCTGCGTCATAGGCTGGGTTGGGTCTAGTGGTTGGGTGTG
PAI-1 04	CGGGGAACACGGGGTGGACGAAGTGGTTGTGTTGGA TGGGAGGGGCA TGTCACCCCTGG
PAI-1 05	CGGGGAACACGGGGTGGACGAAGTGGTTGTGTTGGA TGGGAGGGGCA TGTCACCCCTGG
PAI-1 08	CGGGGAACACGGGGTGGACGAAGTGGTTGTGTTGGA TGGGAGGGGCA TGTCACCCCTGG
PAI-1 09	CGGGGAACACGGGGTGGACGAAGTGGTTGTGTTGGA TGGGAGGGGCA TGTCACCCCTGG
PAI-1 13	CGGGGAACACGGGGTGGACGAAGTGGTTGTGTTGGA TGGGAGGGGCA TGTCACCCCTGG
PAI-1 15	CGGGGAACACGGGGTGGACGAAGTGGTTGTGTTGGA TGGGAGGGGCA TGTCACCCCTGG
PAI-1 16	CGGGGAACACGGGGTGGACGAAGTGGTTGTGTTGGA TGGGAGGGGCA TGTCACCCCTGG
PAI-1 03	CACTTCGATTGTCGTGGAGGTGGGGTAGGGTGAGACCGTGCA TCGGCCG
PAI-1 20	CACTTCGATTGTCGTGGAGGTGGGGTAGGGTGAGACCGTGCA TCGGCCG
PAI-1 06	GACA TGGTGGGTGTGTTGGGGTAGGGCGGGAGGGTTGGTGGTCGGCCTTAAAGGCGC

Clone ID	Selected region (5' to 3')
4-1BB 01	ATCCACGAAGTAGACTGCTAGGTTGGGTAGGGTGGTGACAGTGTCTGGGAAGGCTGCC
4-1BB 02	ATCCACGAAGTAGACTGCTAGGTTGGGTAGGGTGGTGACAGTGTCTGGGAAGGCTGCC
4-1BB 06	ATCCACGAAGTAGACTGCTAGGTTGGGTAGGGTGGTGACAGTGTCTGGGAAGGCTGCC
4-1BB 10	ATCCACGAAGTAGACTGCTAGGTTGGGTAGGGTGGTGACAGTGTCTGGGAAGGCTGCC
4-1BB 12	ATCCACGAAGTAGACTGCTAGGTTGGGTAGGGTGGTGACAGTGTCTGGGAAGGCTGCC
4-1BB 14	ATCCACGAAGTAGACTGCTAGGTTGGGTAGGGTGGTGACAGTGTCTGGGAAGGCTGCC
4-1BB 15	ATCCACGAAGTAGACTGCTAGGTTGGGTAGGGTGGTGACAGTGTCTGGGAAGGCTGCC
4-1BB 07	GTCAGATTCCACTATAGTAGGTTGGGTAGGGTGGTCGCAGTGGATGATAATGTCGTAGGGG
4-1BB 08	GTCAGATTCCACTATAGTAGGTTGGGTAGGGTGGTCGCAGTGGATGATAATGTCGTAGGGG
4-1BB 09	GTCAGATTCCACTATAGTAGGTTGGGTAGGGTGGTCGCAGTGGATGATAATGTCGTAGGGG
4-1BB 11	GTCAGATTCCACTATAGTAGGTTGGGTAGGGTGGTCGCAGTGGATGATAATGTCGTAGGGG
4-1BB 17	GTCAGATTCCACTATAGTAGGTTGGGTAGGGTGGTCGCAGTGGATGATAATGTCGTAGGGG
4-1BB 18	GTCAGATTCCACTATAGTAGGTTGGGTAGGGTGGTCGCAGTGGATGATAATGTCGTAGGGG
4-1BB 19	GTCAGATTCCACTATAGTAGGTTGGGTAGGGTGGTCGCAGTGGATGATAATGTCGTAGGGG
4-1BB 20	GTCAGATTCCACTATAGTAGGTTGGGTAGGGTGGTCGCAGTGGATGATAATGTCGTAGGGG
4-1BB 04	GTCAGATTCCACTATAGTAGGTTGGGTAGGGTGGTCGCAGTGGATGATAATGTCGTAGGGG
4-1BB 16	GTCAGATTCCACTATAGTAGGTTGGGTAGGGTGGTCGCAGTGGATGATAATGTCGTAGGGG
4-1BB 03	GGCGGTGTAATGTGGTTGAGGTGGTGGGGGGCGGGTGGGAGAGGACGAGGCGC
4-1BB 13	GGCGGTGTAATGTGGTTGAGGTGGTGGGGGGCGGGTGGGAGAGGACGAGGCGC
4-1BB 05	ATGTCGAGTAGGTTGGTAGGGTGGTCGTTGATAATCATTTATATCCCTGCTAGTCTGC

**Table S3 | Sequences of best aptamers.**

Clone ID	Selected region (5' to 3')
Thrombin 03	CAG CGC TAGGGCTTTAGCGTAA TGGG TAGGG TGG TG CGG TG CAGA TA TCGGA ATTGGTG
ApoE 06	GAT AAA CG CCTTGATTAAAGGCCAGTTCTTAGGCCTACACG TG CTG CG ACATTAATT
PAI-1 01	CA TGAGATA GCTAGTTGTA GCTGCGTCATAGGCTGGGTTGGGCTAGTGGTTGGGTG
4-1BB 07	GTCAGATTCCACTATAGTAGGTTGGGTAGGGTGGTCG CAGTGGATGATA TGT CGTAGGGG

## References

1. Dressman D, Yan H, Traverso G, Kinzler KW, Vogelstein B (2003) Transforming single DNA molecules into fluorescent magnetic particles for detection and enumeration of genetic variations. *Proc Natl Acad Sci U S A* 100:8817–22. Available at: <http://www.ncbi.nlm.nih.gov/pmc/articles/PMC166396/> [tool=pmcentrez&rendertype=abstract] [Accessed May 3, 2011].
2. Diehl F et al. (2006) BEAMing: single-molecule PCR on microparticles in water-in-oil emulsions. *Nat Methods* 3:551–9. Available at: <http://www.ncbi.nlm.nih.gov/pubmed/16791214> [Accessed May 19, 2011].
3. Ahmad KM et al. (2011) Probing the limits of aptamer affinity with a microfluidic SELEX platform. *PLoS One* 6:e27051. Available at: <http://www.ncbi.nlm.nih.gov/pmc/articles/PMC3215713/> [tool=pmcentrez&rendertype=abstract] [Accessed March 12, 2012].
4. Irvine D, Tuerk C, Gold L (1991) SELEXION. Systematic evolution of ligands by exponential enrichment with integrated optimization by non-linear analysis. *J Mol Biol* 222:739–61. Available at: <http://www.ncbi.nlm.nih.gov/pubmed/1721092> [Accessed July 21, 2011].
5. Wang J, Rudzinski JF, Gong Q, Soh HT, Atzberger PJ (2012) Influence of Target Concentration and Background Binding on In Vitro Selection of Affinity Reagents. *PLoS One* 7:e43940. Available at: <http://dx.plos.org/10.1371/journal.pone.0043940> [Accessed September 4, 2012].
6. Boder ET, Wittrup KD Optimal screening of surface-displayed polypeptide libraries. *Biotechnol Prog* 14:55–62. Available at: <http://www.ncbi.nlm.nih.gov/pubmed/10858036> [Accessed October 1, 2012].
7. Feldhaus MJ et al. (2003) Flow-cytometric isolation of human antibodies from a nonimmune *Saccharomyces cerevisiae* surface display library. *Nat Biotechnol* 21:163–70. Available at: <http://dx.doi.org/10.1038/nbt785> [Accessed August 1, 2012].

8. Herzenberg LA, Tung J, Moore WA, Herzenberg LA, Parks DR (2006) Interpreting flow cytometry data: a guide for the perplexed. *Nat Immunol* 7:681–5. Available at: <http://dx.doi.org/10.1038/ni0706-681> [Accessed July 31, 2012].
9. Bock LC, Griffin LC, Latham JA, Vermaas EH, Toole JJ (1992) Selection of single-stranded DNA molecules that bind and inhibit human thrombin. *Nature* 355:564–6. Available at: <http://dx.doi.org/10.1038/355564a0> [Accessed July 17, 2012].
10. Tasset DM, Kubik MF, Steiner W (1997) Oligonucleotide inhibitors of human thrombin that bind distinct epitopes. *J Mol Biol* 272:688–98. Available at: <http://www.ncbi.nlm.nih.gov/pubmed/9368651> [Accessed October 1, 2012].
11. Zuker M (2003) Mfold web server for nucleic acid folding and hybridization prediction. *Nucleic Acids Res* 31:3406–15. Available at: [http://www.pubmedcentral.nih.gov/articlerender.fcgi?artid=169194&tool=pmcentrz&rendertype=abstract](http://www.pubmedcentral.nih.gov/articlerender.fcgi?artid=169194&tool=pmcentrez&rendertype=abstract) [Accessed August 10, 2012].